J. Fluid Mech. (1991), *vol.* 225, *pp.* 333–354
Printed in Great Britain

Double-diffusive instabilities at a sloping boundary

By O. S. KERR
School of Mathematics, University of Bristol, Bristol BS8 1TW, UK

(Received 9 July 1990)

When a body of fluid with a vertical salinity and temperature gradient is bounded by a sloping boundary, convective instabilities are often observed. These can occur if the fluid is subjected to heating or the addition of solute at the boundary, or if the boundary is an insulator. These instabilities often take the form of long thin convection cells that are almost horizontal. We present a linear stability analysis of the background states associated with these different boundary conditions and derive criteria for their stability in terms of one non-dimensional parameter, Q. This parameter is related to the Rayleigh number and is a generalization of the similar parameter found by Kerr (1989) in his study of heating a salinity gradient from a vertical boundary. This analysis uses a quasi-static assumption that is valid when the vertical lengthscales of the instabilities are less than the horizontal lengthscales.

1. Introduction

When a body of fluid has a vertical density gradient due to either a vertical temperature or salinity gradient, or a combination of the two, and has lateral temperature and salinity gradients, but no horizontal density gradient, instabilities are often observed. It can be shown that if an infinite body of fluid has temperature and salinity gradients that are uniform in every direction then the presence of horizontal compositional gradients always leads to instabilities. This holds for different models of the heat and salt fluxes such as salt fingers (Stern 1967), eddy fluxes (McDougall 1985) and molecular diffusivities (Holyer 1983), although the models with the fluxes dominated by salt fingers and eddy fluxes also require that the vertical gradients have destabilizing salinity gradients. However, when the lateral gradients are bounded in the horizontal direction the fluid may or may not be subject to instabilities. Such localized horizontal gradients that have been examined theoretically fall into three broad classes: (i) instabilities between parallel walls (Thorpe, Hutt & Soulsby 1969; Hart 1971; Paliwal & Chen 1980; Thangam, Zebib & Chen 1981), (ii) localized linear horizontal gradients in infinite fluids (Niino 1986, for the case where the fluxes are dominated by salt fingers) and (iii) localized horizontal gradients near a single boundary (Kerr 1989, for the case of the heating of a semi-infinite salinity gradient from a single vertical sidewall). The object of the present work is to consider some instabilities that lie in this third class. The instabilities examined here are those that occur at a single sloping wall that bounds a body of fluid which has linear vertical temperature and salinity gradients away from the wall. Some examples of this class of instability were observed experimentally by Linden & Weber (1977). They investigated the effect of inserting a sloping boundary into water with vertical sugar and salinity gradients. They found that in some cases instabilities occurred at the boundary, taking the form of nearly horizontal, flat convection cells. Although publications concerning double diffusion

are usually couched in terms of heat and salt, the theory only requires two independent components that affect the density and which have differing diffusivities. By convention the component with the higher diffusivity is referred to as the heat and the component with the lower diffusivity as the salt. Hence for the case of sugar and salt the sugar corresponds to the salt and the salt corresponds to the heat. The convention is adhered to here. The presence of the sloping boundary with no-flux conditions for the sugar and salt leads to a background state with a growing region of localized sugar and salt gradients which have, to leading order, compensating effects on the density (Linden & Weber 1977). It is this region that may sustain instabilities. Another related class of instabilities occurs when, instead of an insulating boundary with a no-flux condition on the heat and salt, the boundary is heated or is the source of a flux of salt. Examples of this type of instability were found experimentally by Chen & Skok (1974) who heated a sloping boundary to a body of water with a vertical salinity gradient. Again there is a growing region near the wall where there are compensating horizontal temperature and salinity gradients.

One application of this analysis is to salt-gradient solar ponds where large pools of water with a stabilizing vertical salinity gradient are used to collect and store solar energy. This results in the water in the ponds having both strong vertical salinity and strong temperature gradients, although stably stratified. The walls of these solar ponds are usually sloping. In addition the walls of the solar ponds may undergo heating due to incident solar radiation. These instabilities could also be relevant to magma chambers where the hot stratified magma is retained by non-vertical walls. It is the instabilities that arise from the two possible sets of boundary conditions, insulating boundaries or heated boundaries, that are examined in this paper. Since we will allow arbitrary slope we will include in these situations the case of heating a combined salinity and temperature gradient from a vertical sidewall. The purpose of this work is to establish when instabilities should be observed and allow the prediction of instabilities in a variety of situations such as the experiments of Linden & Weber, or cases where there is a sloping boundary to a body of fluid with vertical temperature and salinity gradients such as in salt-gradient solar ponds. In §2 we set out the basic background states associated with sloping boundaries with either no-flux conditions for both the heat and salt or for the case where a temperature and salinity difference is imposed at the wall. In §3 we present a linear stability analysis of these background states. It is shown that for the case of no-flux boundary conditions the fluid should always become unstable, and a possible explanation is given as to why instabilities were not always observed by Linden & Weber. The conditions under which instabilities will occur for the case of imposed temperature and salinity differences are also examined in this section. In §4 we look at the influence on the onset of instability of some of the terms in the governing equations that were neglected in the previous section. The leading-order stability of §3 is determined only by the horizontal temperature and salinity profiles. In §4 the first direct effect of the slope angle is determined. In §5 there is a discussion of some of the implications of this work.

Throughout this paper it is assumed that we are looking at the case where the salinity gradient is stabilizing. This conforms with most of the reported experiments, and the motivating physical problems. This means that the situations where there is a destabilizing salinity gradient but a stabilizing temperature gradient are not considered. Such a situation is prone to salt fingering and so the fluxes of heat and salt would tend to be dominated by these salt fingers and not the molecular

diffusivities assumed here. This is the case in some of the experiments of Linden & Weber.

2. Background state

When a sloping boundary which is both an insulator and is impermeable to salt is inserted into a body of fluid with uniform vertical temperature gradient, $\bar{T}_z$, and salinity gradient, $\bar{S}_z$, the isotherms and isopycnals must meet the boundary at right angles. Either gradient in isolation would induce a steady along-wall current (Phillips 1970; Wunsch 1970). However, with the differing diffusivities of salt and heat it is not possible for a steady-state boundary layer to exist (Linden & Weber 1977). Instead a flow ensues which consists of a thin steady boundary layer comprising of an along-wall current with associated temperature and salinity variations, and a thickening region outside this layer where the evolving temperature and salinity perturbations have a balancing effect on the density. We model the fluid as being incompressible and satisfying the Boussinesq approximation, and with a linear equation of state, satisfying the governing equations

$$\frac{\partial \boldsymbol{u}}{\partial t}+\boldsymbol{u}\cdot\nabla\boldsymbol{u}=-\frac{1}{\rho_0}\nabla p+g(\alpha T-\beta S)\,\hat{\boldsymbol{z}}+\nu\nabla^2\boldsymbol{u}, \tag{2.1a}$$

$$\frac{\partial T}{\partial t}+\boldsymbol{u}\cdot\nabla T=\kappa_T\nabla^2 T, \tag{2.1b}$$

$$\frac{\partial S}{\partial t}+\boldsymbol{u}\cdot\nabla S=\kappa_S\nabla^2 S, \tag{2.1c}$$

$$\nabla\cdot\boldsymbol{u}=0, \tag{2.1d}$$

where the density, ρ, is given by

$$\rho=\rho_0(1-\alpha(T-T_0)+\beta(S-S_0)). \tag{2.2}$$

Here ν is the kinematic viscosity, g the acceleration due to gravity, κ_T the diffusivity of heat, κ_S the diffusivity of salt, α the coefficient of thermal expansion and β is the density change due to a unit change in the salinity.

The large-time asymptotic behaviour of the along-wall velocity, and the background temperature and salinity a time t after the introduction of the sloping boundary are found by the use of Laplace transforms (Linden & Weber 1977), to give at leading order

$$\bar{u}=-\hat{\xi}\left(\frac{\kappa_T}{\pi t}\right)^{\frac{1}{2}}\cot\theta\frac{\lambda(1-\tau)^2}{(1-\lambda)^{\frac{1}{2}}(1-\tau\lambda)^{\frac{1}{2}}}\exp\left(-\tfrac{1}{4}A^2\eta^2\right)$$

$$+2\hat{\xi}\cot\theta\frac{\tau(1-\lambda)}{1-\tau\lambda}\kappa_T M\,\mathrm{e}^{-M\eta}\sin M\eta, \tag{2.3a}$$

$$\bar{T}=T_0+z\bar{T}_z+\bar{T}_z\cos\theta\frac{2(1-\tau)(\kappa_T t)^{\frac{1}{2}}}{[(1-\lambda)(1-\tau\lambda)]^{\frac{1}{2}}}\mathrm{ierfc}\left(\tfrac{1}{2}A\eta\right)$$

$$+\bar{T}_z\cos\theta\frac{\tau(1-\lambda)}{1-\tau\lambda}M^{-1}\mathrm{e}^{-M\eta}\cos M\eta, \tag{2.3b}$$

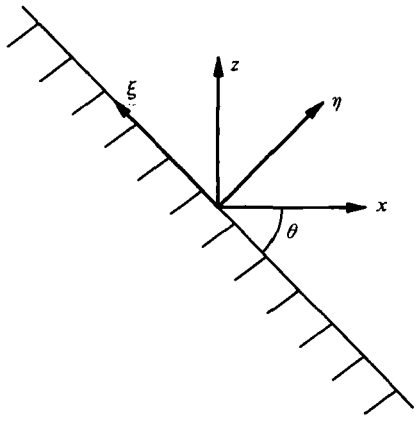

FIGURE 1. Configuration diagram.

and

$$\bar{S} = S_0 + z\bar{S}_z + \frac{\alpha\bar{T}_z}{\beta}\cos\theta\frac{2(1-\tau)(\kappa_T t)^{\frac{1}{2}}}{[(1-\lambda)(1-\tau\lambda)]^{\frac{1}{2}}}\text{ierfc}\,(\tfrac{1}{2}A\eta)$$

$$+\bar{S}_z\cos\theta\frac{1-\lambda}{1-\tau\lambda}M^{-1}\,\mathrm{e}^{-M\eta}\cos M\eta, \quad (2.3c)$$

where $$A^2 = \frac{(1-\lambda)}{(1-\tau\lambda)\kappa_T t}, \quad M^4 = \left(\frac{\alpha\bar{T}_z}{\kappa_T} - \frac{\beta\bar{S}_z}{\kappa_S}\right)\frac{g\sin^2\theta}{4\nu}. \quad (2.4a, b)$$

Here z is the vertical coordinate, η is the perpendicular distance from the boundary, $\hat{\boldsymbol{\xi}}$ the unit vector along the slope, and θ the angle between the boundary and the horizontal. This configuration is shown in figure 1. The other parameters that appear in this expression are the salt/heat diffusivity ratio $\tau = \kappa_S/\kappa_T$ and $\lambda = \alpha\bar{T}_z/\beta\bar{S}_z$. The latter is the ratio of the contribution to the vertical density gradient of the vertical temperature and salinity gradients. The function ierfc is the first integral of the complementary error function.

Instead of having no-flux conditions at the boundary we can consider the case where the body of fluid is subjected to heating and/or addition of solute at the boundary. We will restrict ourselves to the cases where the addition of heat and/or salt is done in such a way that the difference between the temperature and/or solute concentration at the wall differs by a constant amount from the far-field values at the same height. This restriction ensures that the background flow is uniform along the wall. If only heat or salt is added we will assume that the boundary is insulating to the other component. These are idealizations which can be applicable, at least locally, to real situations.

As in the case of heating a pure salinity gradient from a vertical sidewall (Kerr 1989, hereinafter referred to as I), having differences of salinity or temperature that are imposed at some time and are subsequently constant is unrealistic in as much as this cannot happen in practice. It would also violate some aspects of the quasi-static assumptions that will be introduced later. In reality one would expect that the temperature and/or salinity at the wall would evolve to the fixed level steadily and that the fluid would initially be stable, but would become unstable at some later time

when the quasi-static assumptions are valid (see I). However, all the different possible forms of increasing the wall temperature and/or salinity to a fixed level will induce evolving horizontal temperature and salinity gradients in the bulk of the fluid that tend to those found by instantaneously heating the wall temperature and/or salinity, and as such we will use these induced temperature and salinity gradients as representative in much of the analysis relating to the heating or addition of salt at sloping boundaries. For the case where the temperature at the wall is increased by ΔT and the salinity by ΔS the leading-order large-time behaviour is again found by Laplace transforms. The along-wall velocity, and the background temperature and salinity are found to be

$$\bar{u} = -\hat{\xi}\frac{\lambda(1-\lambda)^{\frac{1}{2}}}{(1-\tau\lambda)^{\frac{1}{2}}}\frac{(\alpha\Delta T-\lambda\tau\beta\Delta S)\,\eta}{2\alpha\bar{T}_z(\pi\kappa_T t)^{\frac{1}{2}}}\operatorname{cosec}\theta\exp\left(-\tfrac{1}{4}A^2\eta^2\right)$$

$$+\hat{\xi}\operatorname{cosec}\theta\frac{\lambda\tau(\beta\Delta S-\alpha\Delta T)}{\alpha\Delta T(1-\lambda\tau)}2M^2\kappa_T\,\mathrm{e}^{-M\eta}\sin M\eta, \quad (2.5a)$$

$$\bar{T} = T_0+z\bar{T}_z+\frac{\alpha\Delta T-\lambda\tau\beta\Delta S}{\alpha(1-\tau\lambda)}\operatorname{erfc}\left(\tfrac{1}{2}A\eta\right)+\frac{\lambda\tau(\beta\Delta S-\alpha\Delta T)}{\alpha(1-\lambda\tau)}\mathrm{e}^{-M\eta}\cos M\eta, \quad (2.5b)$$

and

$$\bar{S} = S_0+z\bar{S}_z+\frac{\alpha\Delta T-\lambda\tau\beta\Delta S}{\beta(1-\tau\lambda)}\operatorname{erfc}\left(\tfrac{1}{2}A\eta\right)+\frac{(\beta\Delta S-\alpha\Delta T)}{\beta(1-\lambda\tau)}\mathrm{e}^{-M\eta}\cos M\eta, \quad (2.5c)$$

where A and M are defined as before. The function erfc is the complementary error function.

If, instead of having fixed temperature and salinity differences, we have a fixed temperature difference and a no-flux condition on the salinity then the leading-order large-time along-wall velocity will be similar to the above, but with the application of a temperature difference ΔT at the wall and an effective salinity difference of $\alpha\Delta T/\beta$. The terms corresponding to the boundary layer of thickness M^{-1} will be proportional to $t^{-\frac{1}{2}}$ at leading order.

3. Stability analysis

In this section we perform a linear stability analysis of the background state found in the previous section in a similar fashion to the analysis of I in the investigation of the stability of salinity gradients heated from a single vertical sidewall. In this analysis we will make several assumptions. The first is that the instabilities are driven by the temperature and salinity gradients in the region of the background state that has the temperature and salinity perturbations evolving with a lengthscale growing as $t^{\frac{1}{2}}$. If the instabilities are driven by the boundary layer of thickness M^{-1} then it would be expected that the instabilities would appear when the two lengthscales separate. However, this happens on a typical timescale of order a few seconds whilst the instabilities may take a much longer time to appear. The second, and crucial, assumptions is a quasi-static assumption: we assume that in this stability analysis we can, at least to a first approximation, ignore the time dependency of the external evolving layer. The justification for this is that the instabilities that are observed usually take the form of long thin almost horizontal convection cells. After the onset of instability the growth rate of these convection

cells scales with the diffusion time of heat across the height of the cells, while the evolving background state grows with a timescale of the order of the diffusion time along the length of these cells. Hence, for long, thin, almost horizontal cells the timescale for their growth is much less than the timescale inherent in the evolution of the background. For further discussion see I.

With these assumptions the linearized equations of motion for perturbations to the background state are

$$\frac{\partial \nabla^2 \psi}{\partial t} - (\nabla \psi) \cdot \frac{\partial^2 \bar{\boldsymbol{u}}}{\partial \eta^2} + \bar{\boldsymbol{u}} \cdot \nabla \nabla^2 \psi = g\left(\alpha \frac{\partial T}{\partial x} - \beta \frac{\partial S}{\partial x}\right) + \nu \nabla^4 \psi, \tag{3.1a}$$

$$\frac{\partial T}{\partial t} - \frac{\partial \psi}{\partial z}\frac{\partial \bar{T}}{\partial x} + \frac{\partial \psi}{\partial x}\frac{\partial \bar{T}}{\partial z} + \bar{\boldsymbol{u}} \cdot \nabla T = \kappa_T \nabla^2 T, \tag{3.1b}$$

$$\frac{\partial S}{\partial t} - \frac{\partial \psi}{\partial z}\frac{\partial \bar{S}}{\partial x} + \frac{\partial \psi}{\partial x}\frac{\partial \bar{S}}{\partial z} + \bar{\boldsymbol{u}} \cdot \nabla T = \kappa_S \nabla^2 S, \tag{3.1c}$$

with the stream function defined by

$$(u, w) = \left(-\frac{\partial \psi}{\partial z}, \frac{\partial \psi}{\partial x}\right). \tag{3.1d}$$

We can non-dimensionalize these equations with respect to the following quantities:

$$T \quad \text{with respect to} \quad \Delta T^*, \tag{3.2a}$$

$$S \quad \text{with respect to} \quad \alpha \Delta T^*/\beta, \tag{3.2b}$$

$$x \quad \text{with respect to} \quad L = \left(\frac{1-\tau\lambda}{1-\lambda}\right)^{\frac{1}{2}} \frac{(\kappa_T t^*)^{\frac{1}{2}}}{\sin\theta} = (A \sin\theta)^{-1}, \tag{3.2c}$$

$$z \quad \text{with respect to} \quad H = \frac{(1-\tau)\alpha \Delta T^*}{(1-\tau\lambda)(-\beta \bar{S}_z)}, \tag{3.2d}$$

$$t \quad \text{with respect to} \quad H^2/\kappa_T, \tag{3.2e}$$

$$\psi \quad \text{with respect to} \quad L\kappa_T/H. \tag{3.2f}$$

The horizontal coordinate x is non-dimensionalized with respect to L, the horizontal extent of this outer layer. The vertical coordinate has a different lengthscale, H, in its non-dimensionalization and in our analysis we assume that $H \ll L$. The temperature scale used is ΔT^*, the temperature perturbation at the inside of the evolving outer boundary layer of the background state. For the case of no-flux conditions for both heat and salt this is given by

$$\Delta T^* = \frac{2(1-\tau)\bar{T}_z}{[(1-\lambda)(1-\tau\lambda)]^{\frac{1}{2}}} \left(\frac{\kappa_T t^*}{\pi}\right)^{\frac{1}{2}} \cos\theta. \tag{3.3}$$

For the case of imposed temperature and salinity differences it is given by

$$\Delta T^* = \frac{\alpha \Delta T - \lambda\tau\beta\Delta S}{\alpha(1-\tau\lambda)}. \tag{3.4}$$

For the case of an imposed temperature difference, but no salt flux through the boundary, this term would just be the imposed temperature difference.

The timescale t^* is as yet unspecified. We will anticipate the results of this analysis by choosing for this the time at the onset of instability.

Before writing down the non-dimensional equations for the development of perturbations to these background states it is convenient to change the coordinate system to one in which the vertical coordinate is unchanged, but the horizontal coordinate measures the horizontal distance from the sloping wall to the point of interest. Because of the form that the instabilities take these are a natural choice of coordinates, however they are non-orthogonal.

The linearized non-dimensional governing equations are

$$\frac{\partial \nabla_m^2 \tilde{\psi}}{\partial \tilde{t}} = \frac{\sigma\tau Q}{(1-\tau)}\left(\frac{\partial \tilde{T}}{\partial \tilde{x}} - \frac{\partial \tilde{S}}{\partial \tilde{x}}\right) + \sigma \nabla_m^4 \tilde{\psi}, \tag{3.5a}$$

$$\frac{\partial \tilde{T}}{\partial \tilde{t}} - \frac{\partial \tilde{\psi}}{\partial \tilde{z}} f'(\tilde{x}) - \frac{\lambda(1-\tau)}{(1-\tau\lambda)} \frac{\partial \tilde{\psi}}{\partial \tilde{x}} = \nabla_m^2 \tilde{T}, \tag{3.5b}$$

$$\frac{\partial \tilde{S}}{\partial \tilde{t}} - \frac{\partial \tilde{\psi}}{\partial \tilde{z}} f'(\tilde{x}) - \frac{(1-\tau)}{(1-\tau\lambda)} \frac{\partial \tilde{\psi}}{\partial \tilde{x}} = \tau \nabla_m^2 \tilde{S}, \tag{3.5c}$$

where

$$\nabla_m^2 = \frac{\partial^2}{\partial \tilde{z}^2} + \delta \cot\theta \frac{\partial^2}{\partial \tilde{x}\,\partial \tilde{z}} + \delta^2 \operatorname{cosec}\theta \frac{\partial^2}{\partial \tilde{x}^2}. \tag{3.5d}$$

Here $f'(\tilde{x})$ is the non-dimensional horizontal temperature and salinity gradient. The other non-dimensionalized variables in (3.5) are denoted by tildes. We drop these tildes hereafter. The advection terms due to the background flow are omitted for the sake of clarity. They are of order δ^2 (see below) and play no part in the subsequent analysis. The non-dimensional number Q is given by

$$Q = \frac{(1-\tau)\, g\alpha \Delta T^* H^5}{\nu \kappa_S L^2} \tag{3.6}$$

and is related to a Rayleigh number, but takes into account the effect of the vertical density gradient in determining the aspect ratio of the observed instabilities (see I). For the case of no-flux boundary conditions for both salt and heat Q takes the form

$$Q = \frac{64\lambda^6 (1-\tau)^{12} g(\kappa_T t^*)^2 (-\beta \bar{S}_z) \cos^6\theta \sin^2\theta}{(1-\lambda)^2 (1-\tau\lambda)^9 \pi^3 \nu \kappa_S}, \tag{3.7}$$

while δ, the ratio between the vertical lengthscale and the horizontal lengthscale is given by

$$\delta = \frac{H}{L} = -\frac{\lambda(1-\tau)^2 \sin 2\theta}{(1-\tau\lambda)^2 \pi^{\frac{1}{2}}}. \tag{3.8}$$

The requirement that δ is small will be satisfied when the ratio of the temperature gradient to the salinity gradient, λ, is small. From (3.8) it can be seen that this parameter is also small when λ is very large. However, the large $-\lambda$ cases correspond to situations where the vertical temperature gradient dominates the vertical density gradient. In these cases the theory presented here predicts the onset of instabilities

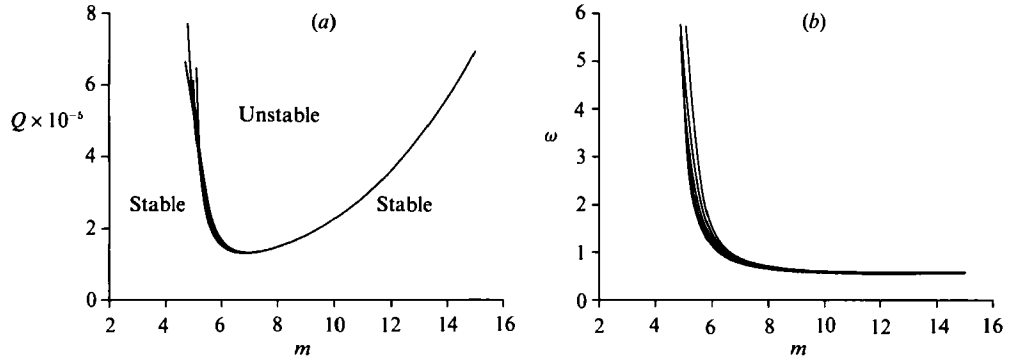

FIGURE 2. Marginal stability curves for a thermally insulating sloping wall that is impermeable to salt for $\sigma = 7$ and $\tau = \frac{1}{80}$, showing (*a*) Q (*b*) the corresponding values of ω as functions of m. In each case curves are shown for $\lambda = -1, -\frac{1}{2}, 0, \frac{1}{2}$ and 1.

for low values of t^*. However, the assumption that the background state is well described by the large-time asymptotics is not then valid. Consideration of these cases is outside the scope of this paper.

For the case of fixed imposed temperature and salinity differences Q takes the form

$$Q = \frac{(1-\tau)^6(1-\lambda)\,g(\alpha\Delta T - \lambda\tau\Delta S)^6 \sin^2\theta}{(1-\tau\lambda)^{12}\nu\kappa_S\kappa_T t^*(-\beta\bar{S}_z)^5}. \tag{3.9}$$

Since none of the coefficients of (3.5) depend on z or t we can look for solutions that are proportional to $\exp\{\mathrm{i}(mz+\omega t)\}$. Neglecting all terms multiplied by δ we can then reduce these equations to the second-order ordinary differential equation for ψ:

$$\psi'' + \frac{\mathrm{i}m^3(1-\tau\lambda)(f'(x)\psi)'}{(\mathrm{i}\omega+m^2)-\lambda(\mathrm{i}\omega+\tau m^2)} - \frac{(1-\tau\lambda)\,m^2(\mathrm{i}\omega+\sigma m^2)(\mathrm{i}\omega+\tau m^2)(\mathrm{i}\omega+m^2)}{[(\mathrm{i}\omega+m^2)-\lambda(\mathrm{i}\omega+\tau m^2)]\sigma\tau Q}\psi = 0. \tag{3.10}$$

This equation further reduces to (3.19) of I in the case $\lambda = 0$. Note that by our choices of the definitions of H, L and Q we no longer have any explicit dependency on the slope angle θ. The results that follow are applicable to slopes of all angles.

The boundary conditions are that ψ vanishes at the wall (correct to leading order) and tends to zero as x tends to infinity. Non-trivial solutions to this eigenvalue problem were found using standard numerical techniques. The far-field boundary condition was modelled by imposing an appropriate radiation condition to allow for the internal waves generated by the translating instabilities. In this way we can find, say, the value of Q and the corresponding value of ω for marginal stability for a given value of m. By varying m the marginal stability curve can be found for any given set of values for σ, τ and λ. The results of this stability analysis will be discussed separately for the different cases of temperature and wall boundary conditions.

3.1. *No-flux conditions for heat and salt*

The marginal stability curves for $\sigma = 7$ and $\tau = \frac{1}{80}$, the approximate values for heat and common salt in water, are shown in figure 2 for several values of λ between -1 and 1. From this we can see that in the case of marginal stability the curves for the values of Q, and the corresponding values of ω, vary by relatively small amounts for

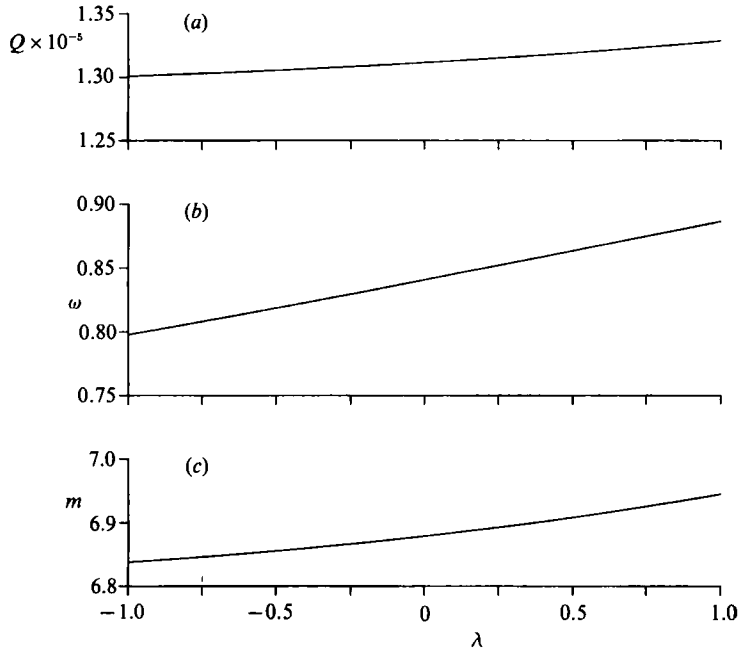

FIGURE 3. Values of (*a*) Q, (*b*) ω, and (*c*) m corresponding to marginal stability for values of λ between -1 and 1 for the case $\sigma = 7$ and $\tau = \frac{1}{80}$, corresponding approximately to the values for heat and salt in water.

significant changes in the buoyancy ratio λ. The values of Q, ω and m corresponding to marginal stability as functions of λ are shown in figure 3. Again there is a relatively small variation in these values with respect to the variation in λ. This lack of variation is a result of the definitions of the vertical lengthscale, H, and of Q. When $\lambda < 0$ both the vertical temperature and salinity gradients are stabilizing, and when $\lambda = -1$ they make the same contribution to the overall density gradient. When $\lambda > 1$ the temperature gradient is destabilizing. In the limit $\lambda = 1$ there is no net vertical density gradient.

Note that by neglecting the $O(\delta)$ terms we cannot apply a no-slip condition at the wall. Similarly the no-flux conditions for the perturbations to the temperature and salinity are lost. If the analysis is extended into the thin steady-state boundary layer and the various regions are matched then these effects can be accounted for. These have an $O(\delta)$ effect on the solution and the values of the parameters for marginal stability. This extension is considered, along with the other previously ignored $O(\delta)$ terms in §4.

In the case of a sloping boundary inserted in water with vertical salinity and sugar gradients a further approximation can be made. In this case $\sigma \approx 560$ and $\tau \approx \frac{1}{3}$ and so we can make a 'large σ' approximation, taking

$$(\mathrm{i}\omega + \sigma m^2) \approx \sigma m^2. \tag{3.11}$$

This enables us to simplify (3.10), obtaining

$$\psi'' + \frac{\mathrm{i}m^3(1-\tau\lambda)(f'(x)\psi)'}{(\mathrm{i}\omega+m^2)-\lambda(\mathrm{i}\omega+\tau m^2)} - \frac{(1-\tau\lambda)m^4(\mathrm{i}\omega+\tau m^2)(\mathrm{i}\omega+m^2)}{[(\mathrm{i}\omega+m^2)-\lambda(\mathrm{i}\omega+\tau m^2)]\tau Q}\psi = 0. \tag{3.12}$$

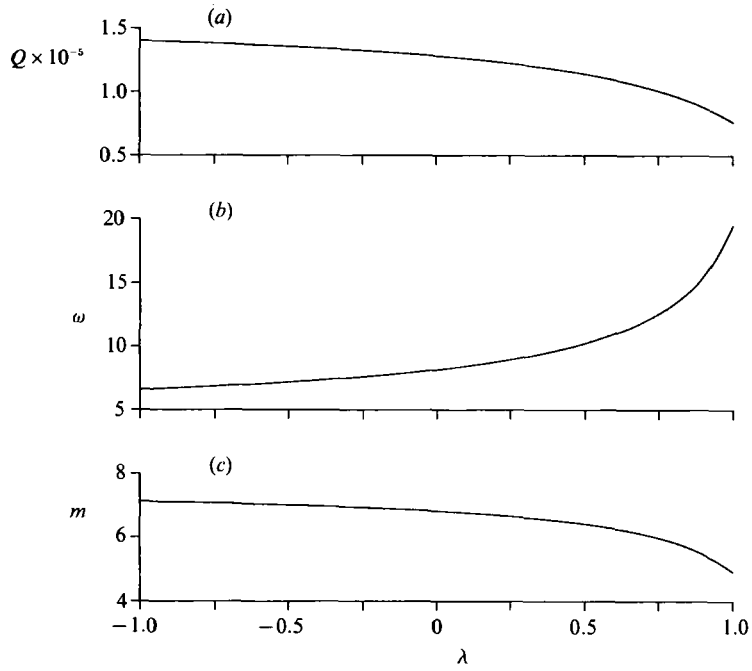

FIGURE 4. Values of (*a*) Q, (*b*) ω, and (*c*) m corresponding to marginal stability for values of λ between -1 and 1 for the case of $\tau = \frac{1}{3}$ using the large-σ approximation.

Again, the boundary conditions are

$$\psi(0) = 0 \quad \text{and} \quad \psi(x) \to 0 \quad \text{as} \quad x \to \infty. \tag{3.13}$$

The critical values of Q for values of λ between -1 and $+1$ can be found for $\tau = \frac{1}{3}$, the approximate value for the sugar/salt system investigated by Linden & Weber (1977). These are shown in figure 4(*a*), with the corresponding values of m and ω shown in figures 4(*b*) and 4(*c*) respectively. This time there is a more marked variation in these quantities as λ varies, especially for λ near to 1.

The form taken by these instabilities is shown in figure 5 for the case of a 45° slope with $\lambda = -0.3$, $\sigma = 7$ and $\tau = \frac{1}{80}$. These show the essentially horizontal nature of the disturbances. For smaller λ these disturbances are even thinner. It should be noted, however, that this linear analysis by its nature predicts counter-rotating convection cells. It has been shown for other related cases of double-diffusive instabilities such as lateral heating of a salinity gradient in a vertical slot (Hart 1973), and the heating of a salinity gradient from a vertical sidewall (Kerr 1990) that the analogous instabilities are subcritical. Also, the sloping-wall experiments reveal corotating convection cells and so it is expected that the counter-rotating cells of this linear analysis will also be subcritical. Hence the nonlinear convection cells that are observed may not correspond closely to these linear instabilities in form.

From (3.7) it can be seen that Q contains a t^{*2} term, with all the other terms fixed at the time of the introduction of the sloping barrier. For any set of parameters the value of Q increases with time, and will eventually reach its critical value. From this we see that the fluid should always become unstable provided the assumptions made in this analysis are valid. The expected time for the onset of instabilities can be calculated from the critical value of Q, and the expected vertical lengthscales of the observed disturbances at the onset of instability. The times taken for the onset of

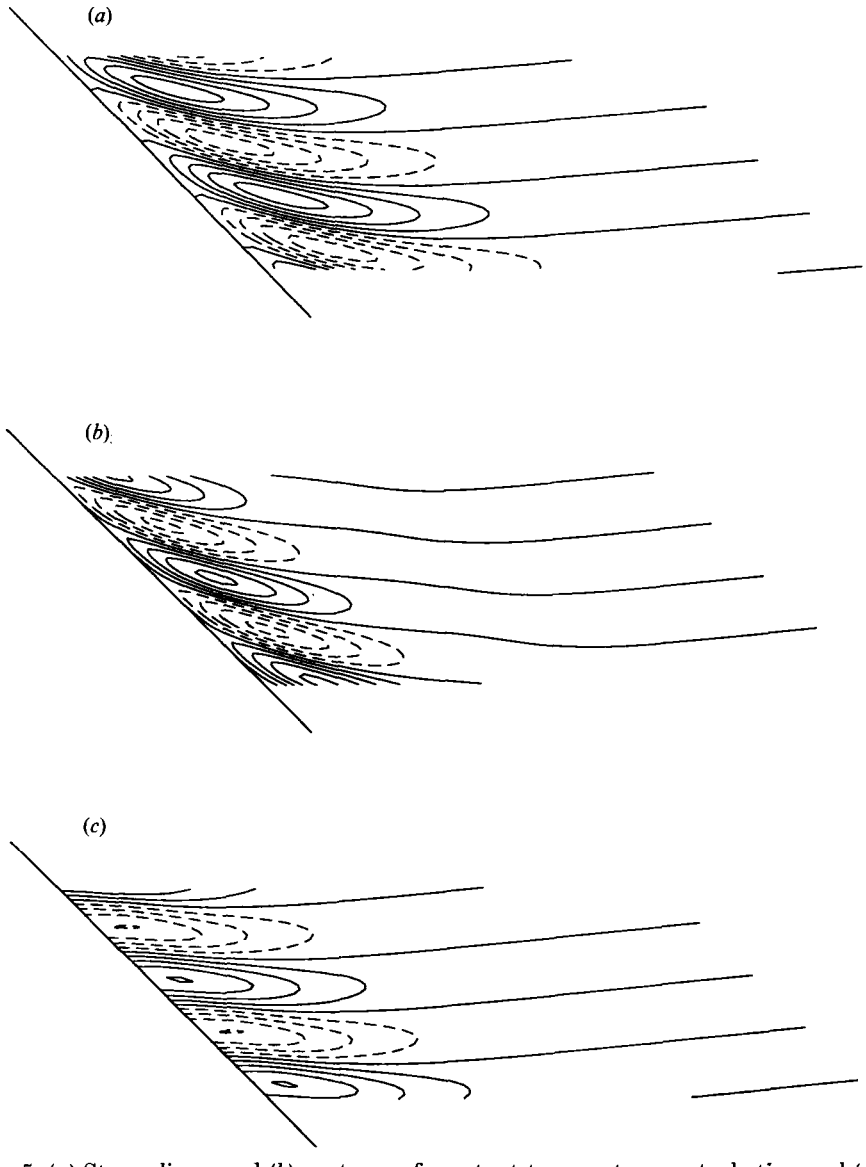

FIGURE 5. (*a*) Streamlines, and (*b*) contours of constant temperature perturbation and (*c*) salinity perturbation for the onset of instability in a heat–salt system with an insulating boundary for x between 0 and 6. In this case $\sigma = 7$ and $\tau = \frac{1}{80}$ for a slope of angle 45° and $\lambda = -0.3$. The intervals between the contours are (*a*) $\Delta\psi = 0.1$, (*b*) $\Delta T = 0.01$, and (*c*) $\Delta S = 0.25$. The negative contours are dashed.

instability, and their vertical lengthscales, in the sugar/salt system are shown in figure 6. It can be seen that the timescale involved increases rapidly as $\lambda \to 0$. Linden & Weber failed to observe any instabilities in their experiments when $\lambda < 0.7$. It can be seen from this graph that this corresponds to a timescale of around five hours. They reported that after this time there were other disturbances that appeared due either to surface effects or to the ends of the slope which disrupted the basic background state. At this point their experiments were terminated.

This theory is valid in the limit of small δ which would correspond to small λ.

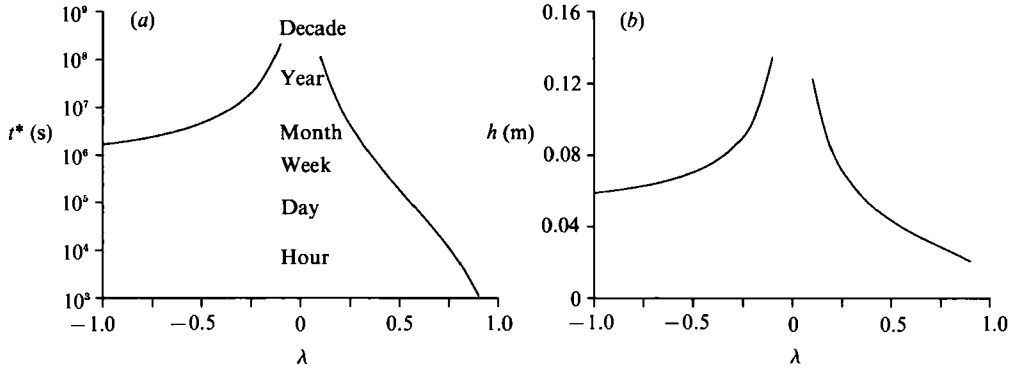

FIGURE 6. (*a*) Time taken, t^*, for the onset of instabilities and (*b*) their height $h = 2\pi H/m$, for an insulating slope of 45° in a salt/sugar system (with $\tau = \frac{1}{3}$ using the large-σ approximation) for λ between −1 and 1.

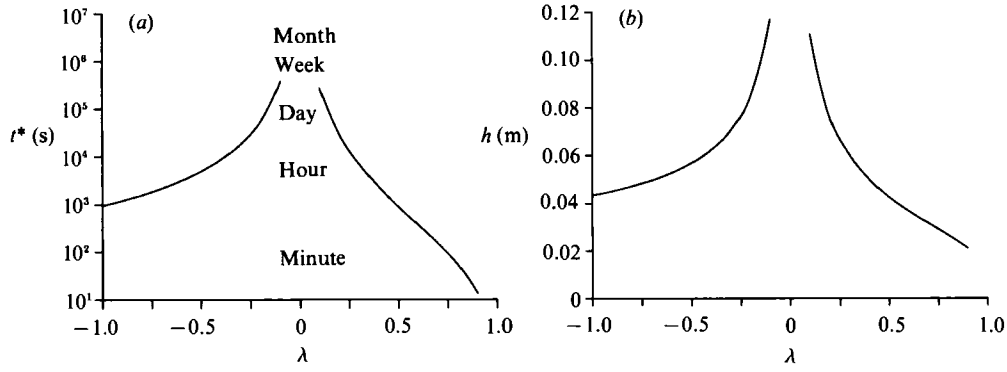

FIGURE 7. (*a*) Time taken, t^*, for the onset of instabilities and (*b*) their height, $2\pi H/m$, for a slope of 45° for a heat/salt system (with $\tau = \frac{1}{80}$ and $\sigma = 7$) for λ between −1 and 1.

However, for a reasonably small value of λ, say $\lambda = \pm 0.1$, the onset of instabilities would be expected after almost a decade, and so it is not surprising that no such instabilities were observed. However, for small λ, Q can be increased, and the onset of instability hastened, by having a stronger salinity stratification (often impractical), setting the slope angle to $\theta = 30°$, or using a fluid and salt whose product of Prandtl number with salt/heat diffusivity ratio is small. For example sugar/salt has $\sigma\tau \approx 200$ while heat/salt has $\sigma\tau \approx 0.9$. Since the value of Q corresponding to the onset of instability is relatively insensitive to changes in the Prandtl number and the salt/heat diffusivity ratio we can see that for the same values of λ, buoyancy frequency etc. the time taken for the onset instability would be approximately 45 times shorter for a heat/salt experiment than for a salt/sugar experiment. This is shown by examination of the time to the onset of instability for water with vertical temperature and salinity gradients (figure 7). From this we can see that using temperature and salt would give a more practical timescale. Alternatively, by using a solute with a much lower diffusivity than sugar as the basic stratifying component the product $\sigma\tau$, and hence the time for the onset of instability, would be much reduced.

By the choice of the vertical lengthscale H and the definition of Q the solutions are well behaved as λ passes through zero. If λ were zero this would correspond to the

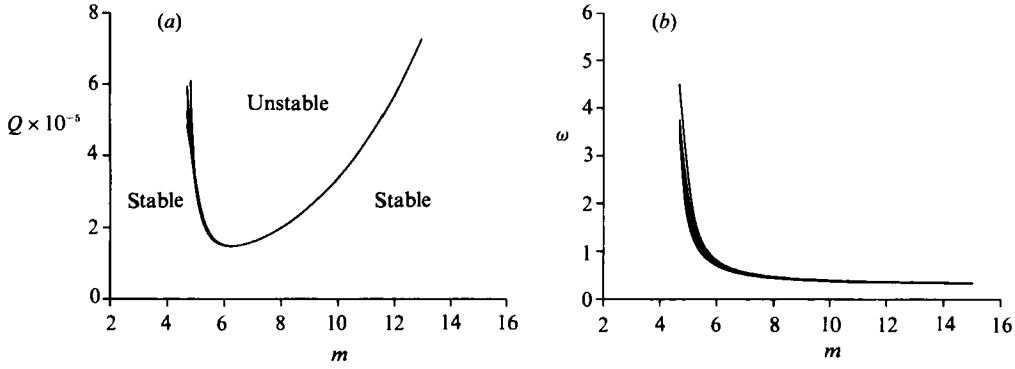

FIGURE 8. Marginal stability curves for an impulsively heated and salted sloping wall for $\sigma = 7$ and $\tau = \frac{1}{80}$, showing (*a*) Q and (*b*) the corresponding values of ω as functions of m. In each case curves are shown for $\lambda = -1, -\frac{1}{2}, 0, \frac{1}{2}$ and 1.

case where no temperature and salinity gradients were present away from the wall. With no such gradients this case would be stable to linear perturbations of the form that we have been seeking. The finite value of Q for marginal instability does not contradict this. There is a factor of λ^6 in the numerator of the definition of Q, so if $\lambda = 0$ then $Q = 0$. As $\lambda \to 0$ this result tells us that, since the critical value of Q remains finite, so t^* must increase as λ^{-3} and so the expected time for onset of instabilities becomes infinite. Also, by the inclusion of the $(1-\tau)$ factors in the definitions of Q and H, the singularity in the equations is removed in the limit $\tau \to 1$. This limit is equivalent to the case where there is only one stratifying component, and corresponds to the Phillips and Wunsch flow. The background perturbation is confined to the steady inner boundary layer. Again there is no contradiction that a finite value of Q is predicted for instability as there is a $(1-\tau)^{12}$ term in the definition of Q which would imply that as $\tau \to 1$ the time taken before the onset of instability increases as $(1-\tau)^{-6}$.

3.2. *Imposed temperature and salinity difference*

When there is an imposed lateral temperature and salinity difference we again obtain the equation for the stream function (3.10). However, there is a different temperature profile. For the case of instantaneously imposed temperature and salinity differences, with the associated error function profiles, we can obtain the critical values of Q as functions of m and the corresponding values of ω as before. These are shown in figure 8 for the case $\sigma = 7$ and $\tau = \frac{1}{80}$ for values of λ between -1 and 1. These results are similar to those obtained for the insulating impermeable boundary considered earlier and again show little variation for different values of λ.

The formulation of this problem in terms of the instantaneous increase in the wall temperature leads to the same problems as discussed in I for the instantaneous heating of a salinity gradient from a vertical sidewall. If the wall temperature and salinity were raised instantaneously to some level and kept there then the resulting value of Q would be proportional to t^{-1}, initially unbounded and decaying to zero. The value of δ would behave similarly. This initially infinite Q would imply instantaneous instability if the quasi-static assumption were not broken along with the assumption of small δ. However, for more realistic imposed increases in the wall temperature and salinity there would be an initial almost linear rise in the wall temperature and salinity, indicating that the instantaneous values of Q would be

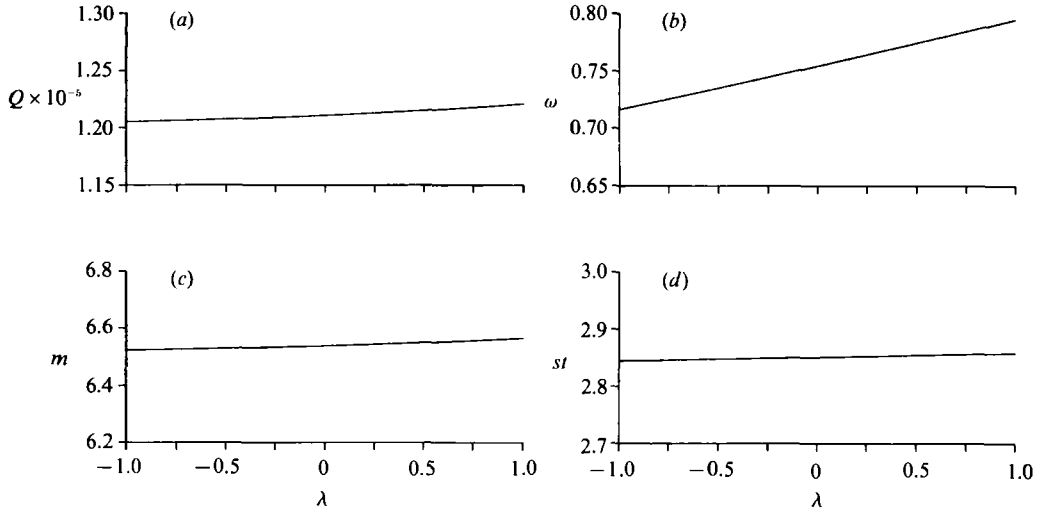

FIGURE 9. Values of (*a*) Q, (*b*) ω, and (*c*) m corresponding to marginal stability for Chen *et al.* (1971) style heating for values of λ between -1 and 1 for the $\sigma = 7$ and $\tau = \frac{1}{80}$, along with the values of (*d*) st corresponding to these points of marginal stability.

proportional to t^5. The fluid would then start in a stable regime and may become unstable later. Reasonable results may be obtained if the error-function temperature profile is used to find the critical values of Q and m and these are then compared to the instantaneous value of Q found when $\Delta T^{*6}/t$ is maximized. However, this does not take into account the changing shape of the temperature and salinity profiles as they evolve from those where ΔT and ΔS are both proportional to t to those where the error function profile is assumed. Instead we will use more realistic wall temperatures and salinities (cf. Chen, Briggs & Wirtz 1971) such as

$$T_{\text{wall}} = \Delta T(1-\mathrm{e}^{-st}), \tag{3.14a}$$

and

$$S_{\text{wall}} = \Delta S(1-\mathrm{e}^{-st}), \tag{3.14b}$$

where s is the rate of evolution of the wall temperature and salinity to their final levels. For the sake of simplicity we have assumed that the wall temperature and wall salinity evolve in the same way over the same timescale. The evolving temperature and salinity profiles outside the thin wall boundary layers are then

$$T(\eta,z,t) = T_0 + z\bar{T}_z + \frac{\alpha\Delta T - \lambda\tau\beta\Delta S}{\alpha(1-\tau\lambda)}(\operatorname{erfc}[\tfrac{1}{2}A\eta] - \mathrm{e}^{-st}\,Re\{\exp(\mathrm{i}(stA^2\eta^2)^{\frac{1}{2}})\operatorname{erfc}[\tfrac{1}{2}A\eta + \mathrm{i}(st)^{\frac{1}{2}}]\}), \tag{3.15a}$$

$$S(\eta,z,t) = S_0 + z\bar{S}_z + \frac{\alpha\Delta T - \lambda\tau\beta\Delta S}{\beta(1-\tau\lambda)}(\operatorname{erfc}[\tfrac{1}{2}A\eta] - \mathrm{e}^{-st}\,\mathrm{Re}\{\exp(\mathrm{i}(stA^2\eta^2)^{\frac{1}{2}})\operatorname{erfc}[\tfrac{1}{2}A\eta + \mathrm{i}(st)^{\frac{1}{2}}]\}), \tag{3.15b}$$

We can now calculate the instantaneous values of Q_{crit}, the value of Q for marginal stability, and the instantaneous values of Q as functions of time. If the curves intersect then the fluid will be unstable to infinitesimal perturbations. Marginal stability will correspond to the case where the two curves touch tangentially (see I). The values of st at which these curves touch for values of λ between -1 and 1 are

shown in figure 9(*d*) along with the corresponding values of Q and the corresponding values of m and ω for the case $\sigma = 7$ and $\tau = \frac{1}{80}$ (figures 9*a–c*). The values of m and ω presented were found using the final wall temperature and salinity in their scalings, not the instantaneous values. From these results it can be seen that over the range of λ shown the value of Q_{crit} and the corresponding values of m vary by a very small amount, whilst ω varies by a larger, but still small, amount. The variation in st corresponding to marginal stability is small over the range of λ shown.

4. Second-order effects

The terms neglected by assuming that $\delta \approx 0$ in the analysis of the previous section were at most $O(\delta)$. The terms that remained were those that would be present for the analysis of the instabilities at a vertical wall. The influence of the boundary slope was purely in the setting up of the background state. It is the neglected terms that convey the direct effect of the slope of the boundary on the instabilities. At this order the effects of the thin boundary layer that did not appear in the previous analysis, and the effect of the neglected horizontal diffusion now appear. These include, for example, the influence of having a no-slip condition at the wall. These effects give $O(\delta)$ corrections to the critical values of Q found for marginal stability. Unlike I, where the first corrections to Q were $O(\delta^2)$, these corrections are of lower order than the $O(\delta^2)$ uncertainty inherent in the quasi-static assumption. In this case the $O(\delta)$ corrections are of physical significance. However, since the form of this perturbation is dependent on the precise boundary conditions and the exact form of the wall heating imposed we will restrict ourselves to the case with the no-flux conditions for both heat and salt. Results obtained for wall heating/salting would not have any degree of generality, and so are not included.

This analysis follows the higher-order analysis of §5 of I closely, and much of the detail is omitted here.

By ignoring the effects of the $O(\delta)$ terms in the leading-order equations we were unable to satisfy the no-slip boundary condition. In the investigation to this order we have to take this effect into account. To do this we must perform a boundary-layer analysis which involves using matched asymptotics between the outer layer that we have been concerned with in §3 and two thinner layers of relative thickness $O(\delta)$ and $O(\delta^{\frac{3}{2}})$. This analysis yields the relationship between the leading-order solution in the outer layer as it tends towards the boundary and the higher-order approximations. It gives an $O(\delta)$ correction to ψ at the wall end of the outer layer. This, combined with the $O(\delta)$ terms in (3.5), leads to expanding the stream function and the temperature and salinity perturbations in the outer layer as asymptotic series in δ. This we also do with Q and ω, giving

$$(\psi(x), T(x), S(x)) = \sum_{j=0}^{\infty} \delta^j (\psi_j(x), T_j(x), S_j(x)), \tag{4.1a}$$

and

$$(Q, \omega) = \sum_{j=0}^{\infty} \delta^j (Q_j, \omega_j). \tag{4.1b}$$

These expansions were substituted into the governing equations and the terms of similar order were collected. The $O(1)$ equations are the leading-order equations given by (3.5) with the higher-order terms ignored. These equations have the solutions found in the previous section, made under the assumption that all $O(\delta)$ terms were negligible. Hence Q_0 and ω_0 will correspond to the critical values found

there. Again we look for solutions that are proportional to $\exp\{\mathrm{i}(mz+\omega t)\}$. From the $O(\delta)$ terms we have

$$m^2(\mathrm{i}\omega_0+\sigma m^2)\psi_1+\frac{\sigma\tau Q_0}{(1-\tau)}\left(\frac{\partial T_1}{\partial x}-\frac{\partial S_1}{\partial x}\right)=-\mathrm{i}\omega_1 m^2\psi_0$$

$$-\frac{\sigma\tau Q_1}{(1-\tau)}\left(\frac{\partial T_0}{\partial x}-\frac{\partial S_0}{\partial x}\right)-2\omega_0 m\cot\theta\frac{\partial\psi_0}{\partial x}+4\sigma\mathrm{i}m^3\cot\theta\frac{\partial\psi_0}{\partial x}, \quad (4.2a)$$

$$(\mathrm{i}\omega_0+m^2)T_1-\mathrm{i}m\psi_1 f'(x)-(1-\tau)\lambda\frac{\partial\psi_1}{\partial x}=-\mathrm{i}\omega_1 T_0+2\mathrm{i}m\cot\theta\frac{\partial T_0}{\partial x}, \quad (4.2b)$$

$$(\mathrm{i}\omega_0+\tau m^2)S_1-\mathrm{i}m\psi_1 f'(x)-(1-\tau)\frac{\partial\psi_1}{\partial x}=-\mathrm{i}\omega_1 S_0+2\tau\mathrm{i}m\cot\theta\frac{\partial S_0}{\partial x}. \quad (4.2c)$$

These equations do not in general have a solution. To find the values of Q_1 and ω_1 for which solutions exist we apply a solvability condition analogous to that used in the $O(\delta^2)$ analysis of I. We multiply (4.2) by the respective conjugates of the adjoints of the $O(1)$ equations, $\hat{\psi}$, $\hat{T}$ and $\hat{S}$, and integrate the sum of these expressions from $x=0$ to ∞. In this way we obtain, after some manipulation, the relationship

$$\begin{aligned}(1-\tau)&(\mathrm{i}\omega_0+m^2)(\mathrm{i}\omega_0+\tau m^2)\psi_1(0)[\lambda\bar{\hat{T}}(0)+\bar{\hat{S}}(0)]\\
&=\frac{m^2Q_1}{Q_0}(\mathrm{i}\omega_0+\sigma m^2)(\mathrm{i}\omega_0+m^2)(\mathrm{i}\omega_0+\tau m^2)\int_0^\infty\bar{\hat{\psi}}\psi_0\,\mathrm{d}x\\
&\quad-\mathrm{i}\omega_1\left\{m^2[(\mathrm{i}\omega_0+\sigma m^2)(\mathrm{i}\omega_0+m^2)+(\mathrm{i}\omega_0+m^2)(\mathrm{i}\omega_0+\tau m^2)\right.\\
&\quad\left.+(\mathrm{i}\omega_0+\tau m^2)(\mathrm{i}\omega_0+\sigma m^2)]\int_0^\infty\bar{\hat{\psi}}\psi_0\,\mathrm{d}x+\frac{\sigma\tau Q_0(1-\lambda)}{(1-\tau\lambda)}\int_0^\infty\bar{\hat{\psi}}'\psi_0'\,\mathrm{d}x\right\}\\
&\quad+2\mathrm{i}m\cot\theta\left\{m^2[3\sigma\tau m^4-2\mathrm{i}(\sigma\tau+\sigma+\tau)\omega_0 m^2-(\sigma+\tau+1)\omega_0^2]\int_0^\infty\bar{\hat{\psi}}\psi_0'\,\mathrm{d}x\right.\\
&\quad\left.-\mathrm{i}\omega_0\frac{\sigma\tau Q_0(1-\lambda)}{(1-\tau\lambda)m^2}\int_0^\infty\bar{\hat{\psi}}'\psi_0'\,\mathrm{d}x\right\}. \quad (4.3)\end{aligned}$$

The analysis of the thin boundary layers yields the relationship between ψ_0 and ψ_1 in the outer layer

$$\psi_1(0)=-\frac{\mathrm{i}\tau m}{M}\frac{(\mathrm{i}\omega_0+m^2)-\lambda(\mathrm{i}\omega_0+\tau m^2)}{(\mathrm{i}\omega_0+\tau m^2)(\mathrm{i}\omega_0+m^2)(1-\tau\lambda)}\cot\theta\,\psi_0'(0). \quad (4.4)$$

A similar analysis for the case of a heated boundary would also yield an expression at this order, again with a $\cot\theta$ factor. Since this term vanishes when the wall is vertical this result, which gives an $O(\delta)$ perturbation at leading order, is consistent with the vertical-sidewall analysis of I which gave an $O(\delta^2)$ perturbation at leading order.

When (4.3) and (4.4) are combined along with the relationship between the adjoints

$$\frac{\sigma\tau Q_0}{(1-\tau)}\hat{\psi}'(0)=(-\mathrm{i}\omega_0+m^2)\hat{T}(0)=-(-\mathrm{i}\omega_0+\tau m^2)\hat{S}(0) \quad (4.5)$$

we obtain an expression involving only $\psi_0(x)$ and its adjoint $\hat{\psi}(x)$. Taking real and imaginary parts of this expression yields two simultaneous equations for Q_1 and ω_1. The terms in these expressions can be calculated numerically, and the solutions

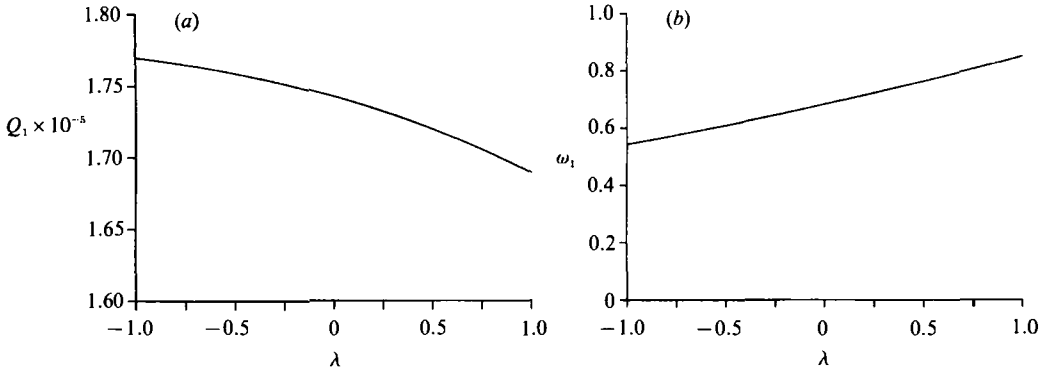

FIGURE 10. The $O(\delta)$ corrections (*a*) Q_1 and (*b*) ω_1 for values of λ between -1 and 1 for the case of $\sigma = 7$ and $\tau = \frac{1}{80}$.

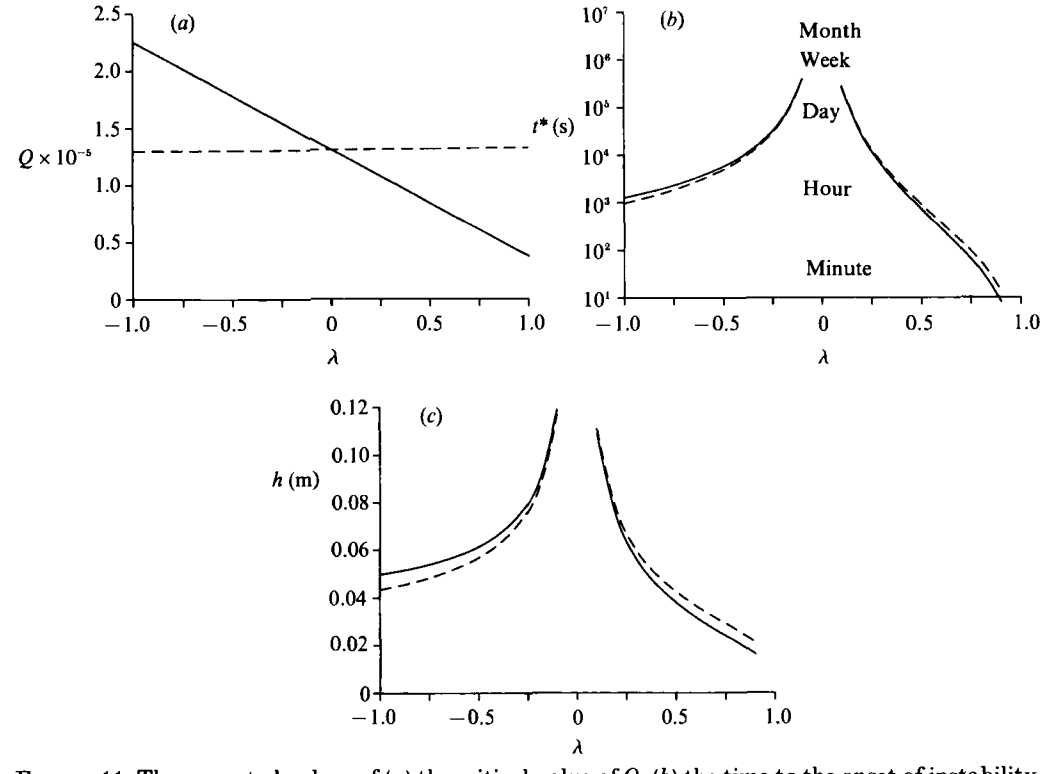

FIGURE 11. The corrected values of (*a*) the critical value of Q, (*b*) the time to the onset of instability, t^*, and (*c*) the height of the instability, $h = 2\pi H/m$, for a thermally insulating slope with angle 45° which is impermeable to salt. These are calculated for λ between -1 and 1 for $\sigma = 7$ and $\tau = \frac{1}{80}$. The uncorrected values are shown as the dashed lines.

found. The results for the case $\sigma = 7$ and $\tau = \frac{1}{80}$ are shown in figure 10. These values can then be used to find the corrected values of Q_{crit} and t^*, with allowance taken for the angle of the slope. Some results are shown in figure 11 for a slope with angle $\theta = 45°$. For an overhanging slope, with $\frac{1}{2}\pi < \theta < \pi$, the signs of Q_1 and ω_1 both change owing to the change in sign of the $\cot\theta$ terms in (4.3) and (4.4). There is also a change in the sign of δ due to the $\sin 2\theta$ term in (3.8) and so the net result is that the modification to the stability is the same for a slope of angle θ and a slope of angle

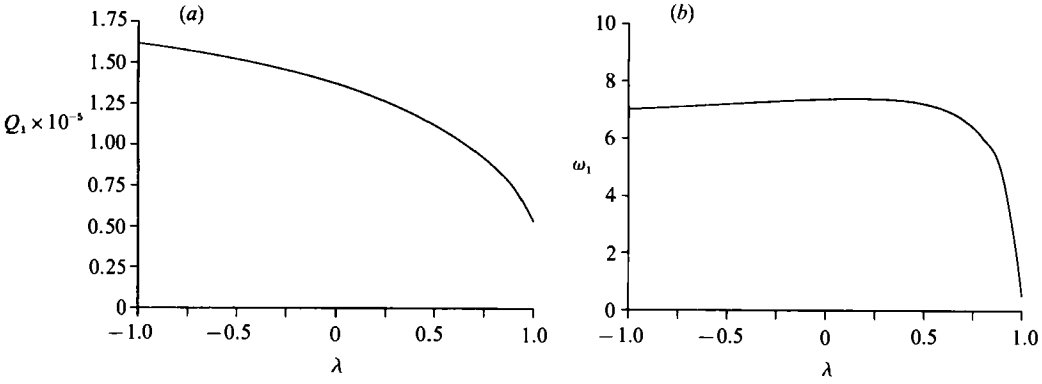

FIGURE 12. The $O(\delta)$ corrections (*a*) Q_1 and (*b*) ω_1 for values of λ between -1 and 1 for the case $\tau = \frac{1}{3}$ calculated using the large-σ approximation.

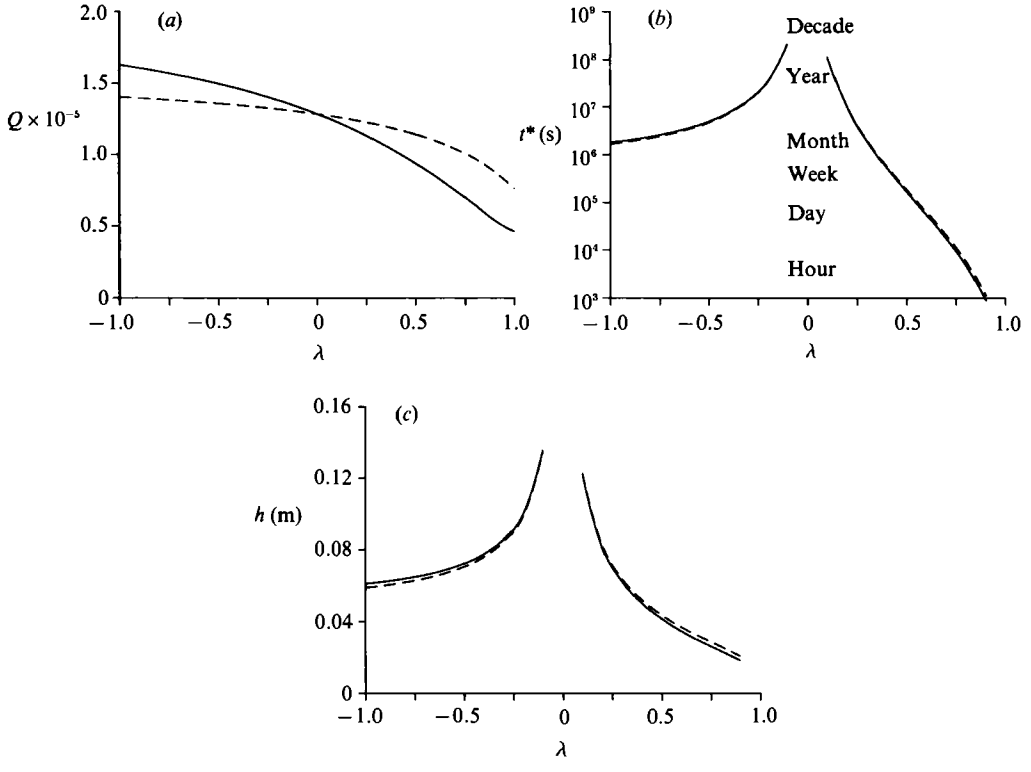

FIGURE 13. The corrected values of (*a*) the critical value of Q, (*b*) the time to the onset of instability, t^*, and (*c*) the height of the instability, $h = 2\pi H/m$, for a slope with angle 45° which is impermeable to both sugar and salt. These are calculated for λ between -1 and 1 for $\tau = \frac{1}{3}$ using the large-σ approximation. The uncorrected values are shown as the dashed lines.

$\pi - \theta$. This implies that if a thin sloping boundary were inserted into a tank then the instabilities should form on the underside at the same time as the top.

The large-σ approximation used to derive (3.12) can also be applied to the determination of Q_1 and ω_1 in appropriate cases. Results using this approximation are shown in figure 12 for $\tau = \frac{1}{3}$, the approximate value for the ratio of the diffusivities of sugar and salt. Again using this approximation, the modified values

of the critical value of Q and the time taken for the onset of instability are shown in figure 13 for $\tau = \frac{1}{3}$.

5. Discussion

In this paper it has been shown that when a fluid with vertical temperature and salinity gradients, with the salinity gradient dominating, is in contact with a sloping boundary then an unsteady background state ensues. This background state has an evolving outer layer of thickness proportional to $t^{\frac{1}{5}}$ where the temperature and salinity perturbations from the basic stratification have counter-balancing effects on the density. We have shown that the stability, under certain approximations, is governed by the non-dimensional number

$$Q = \frac{(1-\tau)\, g\alpha\Delta T^* H^5}{\nu\kappa_S L^2}, \tag{5.1}$$

where ΔT^* is the temperature perturbation at the inside of this evolving outer layer, L the horizontal extent of this layer, and H the vertical lengthscale $(1-\tau)\,\alpha\Delta T^*[(1-\tau\lambda)(-\beta\bar{S}_z)]$. When Q exceeds a number of order 10^5 the fluid becomes unstable to thin almost horizontal convection cells. These results hold when both $\delta = H/L$ and λ are small. This holds for both the case $\lambda > 0$, when the background vertical temperature is destabilizing, and for $\lambda < 0$, when both the background vertical temperature and salinity gradients are stabilizing.

These conditions were not both satisfied in the experiments of Chen & Skok (1974). They heated a pure salinity gradient from a sloping boundary, so $\lambda = 0$. However, owing to the relatively short timescale for the heating up of their wall (~ 2 minutes) δ was not small. Their experiment no. 1 has $\delta \approx 0.6$, and the rest have $\delta > 0.7$. Although both experiments nos. 1 and 2 were subcritical, the value of Q for the second of these was about four times greater than that predicted for marginal stability. Comparison with the experimental results of Tsinober & Tanny (1986) for heating a salinity gradient from a single sidewall (see I) gives two possible reasons for this. The first is that for these larger values of δ the salinity gradients do seem to be significantly more stable than the linear analysis with the quasi-static assumption predicts. Secondly, the large variations in the salinity concentration in the tank mean that the linearized equation of state assumed, (2.2), does not hold globally. It was found in I that the local values of Q calculated along the wall could vary by a factor of 10 between the top of the tank and the bottom of the tank. This leads to instabilities appearing lower down in the experimental tank first and then apparently moving upwards. Such behaviour was also observed by Chen & Skok. This problem can be overcome by using a local stability criterion such as used by Tsinober & Tanny in their experiments. Similarly the results of Linden & Weber cannot provide confirmation of the predictions of this theory. They were unable to address the small-λ limit in their study owing to the breakdown of the background state which arose from other effects associated with the finite extent of their tank. This occurred before the instabilities could appear.

How may these results be applied to more practical considerations? In salt-gradient solar ponds (see Schladow & Imberger 1987) the values of λ lie between about $\frac{1}{3}$ and $\frac{2}{30}$. If the walls were perfect insulators then the onset of instabilities would be expected to occur somewhere between several hours to over a week. However, this may be unimportant compared to the relatively fast heating of the sloping walls of

the solar ponds by direct sunlight. This causes the wall temperature to rise by a few degrees in around half an hour. In this case, for typical temperature and salinity gradients we would expect instability to occur almost universally with a vertical lengthscale of around a centimetre. As Schladow & Imberger reported, there has been little direct observation of solar ponds at sufficient resolution to detect these instabilities. However, their numerical simulations of solar ponds showed that the inclusion of effects of double-diffusive instabilities at the boundaries was needed in order to successfully model the behaviour of solar ponds. It is hoped that present work will improve the understanding of how these mechanisms operate.

The other physical problem which motivated this work was the possible initiation of convective instabilities in the magma at the sloping boundaries of magma chambers. Direct application of the theory is hindered by lack of accurate knowledge of the exact parameters that are appropriate, combined with a far more complicated geometry than the idealized problems studied. However, by use of sensible guesses we can hope to get an idea of the scales of the problem, and to find out whether sidewall instabilities driven by double-diffusive effects could be responsible for some of the convection and mixing that occurs in magma chambers. The compositional variation and the chemistry of the magma are more complicated than can be allowed for in this analysis, so the guesses must include simplifying assumptions. It was assumed that the magma chamber was 10^3 m high with a temperature of 800 °C at the top and of 1200 °C at the bottom. The enclosed magma was stratified, with the density varying from 2.2×10^3 kg m^{-3} at the top to 2.7×10^3 kg cm^{-3} at the bottom. This density gradient would be almost entirely due to compositional gradients, giving a value of $\beta \bar{S}_z \approx -2 \times 10^{-4}$ m^{-1}. The coefficient of thermal expansion was taken to be $\alpha = 10^{-5}$ C^{-1}, giving $\lambda = 2 \times 10^{-2}$. Since this value is small we could expect the analysis in this paper to be appropriate. The diffusivity of temperature was taken to be $\kappa_T = 8 \times 10^{-7}$ m^2 s^{-1}. It was further assumed that the variation in the density between the magma at the base of the chamber and the top is due principally to variations in the SiO_2 concentration. This has a diffusivity $\kappa = 10^{-14}$–10^{-16} m^2 s^{-1}. The other component of the magma which could have a bearing on the dynamics of the magma is the water content. The variation in water concentration may be great at the walls where the melting chamber walls will contain no water compared to a 2–6% water concentration in the bulk magma. Thus at the boundaries we could consider the possibility of convection due to either a heat/SiO_2, or a water/SiO_2 system. In either case the effect of the water concentration is important as it has a strong effect on the viscosity of the magma. The diffusivity of water was taken to be $\kappa = 10^{-11}$ m^2 s^{-1}. The dynamic viscosity can vary considerably, with the viscosity of the basalt influx at the base of the chamber being as low as 10^2 Pa s while the viscosity of the magma at the top of the chamber could vary vetween 10^{11} Pa s and 10^5 Pa s depending on the water content.

We now come to the problem of which set of boundary conditions are the most appropriate to the magma chamber walls. We can consider the effect of an insulating boundary on the magma. This is not entirely appropriate for a heat/SiO_2 system as the diffusivity of heat in the magma is comparable with the diffusivity of heat in the surrounding rocks. However, it could be appropriate for a water/SiO_2 system. With the walls of the magma chamber being cooled and melting it could also be appropriate to use the analysis of the effect of increasing the wall temperature and solute concentration by a fixed amount at the wall. This has the difficulty that the appropriate concentrations and compositional differences that should be used are not clear, nor is the appropriate timescale for the heating up of the wall. With these

difficulties in mind we will make some guesses that seem reasonable in order to get an idea of the likely scales of the non-dimensional parameters.

With the above assumptions, we can calculate the time taken for the onset of instability for an insulating boundary with a slope of 45°. For magma with a viscosity of 10^7 Pa s instability will occur after around 200 years. With each increase in the viscosity by a factor of 100 this time increases by a factor of 10. For less viscous magmas this time would be diminished. These shorter times are plausible and so this should be considered as a possible driving mechanism for convection in magma chambers containing less viscid magmas. However, if we consider the case of no-flux conditions on both water and SiO_2 we find that the time needed for the onset of instability can be of order 10^9 years. This is obviously too long and so can be discounted as a mechanism for instability.

The second kind of instability, that with fixed temperature and compositional differences imposed between the bulk of the magma and the boundary, has to be treated differently. The appropriate differences in temperature and composition are not known with any precision, nor do we have an exact form of their temporal evolution. However, we can make estimates of the typical temperature and compositional differences that may be expected and find from these a timescale for marginal stability. If the differences are imposed on a shorter timescale then we would expect instability to appear. For an imposed temperature difference and a no-flux condition on the salinity we find that a typical timescale for the onset of instability is

$$t^* = \frac{g(\alpha\Delta T)^6 \sin^2\theta}{\nu\kappa_S\kappa_T Q(-\beta\bar{S}_z)^5}. \tag{5.2}$$

We have assumed here that since $\lambda \approx 0.02$ and that τ is small we can ignore the terms involving these quantities. In a similar way the corresponding lengthscale is $(\kappa_T t^*)^{\frac{1}{2}}/\sin\theta$. If instabilities were to exist then they would be expected to be on a lengthscale similar to this, if not shorter. This expression (5.2) can be applied to a variety of cases. For a relatively inviscid magma with viscosity 10^2 Pa s, with a temperature difference of only 1 °C imposed at a boundary of slope 45°, then instabilities would be observed if the heating (or cooling) time was less than about 40 days. The corresponding lengthscale is about $2\frac{1}{2}$ m. If the times were much less than 40 days the driving force of the instabilities would be far from marginal stability, and the convection could be expected to be vigorous. For greater temperature differences this time is greatly increased, as is the lengthscale, as the critical time scales as ΔT^6.

For more viscous magmas the critical time is reduced dramatically. For a magma with viscosity 10^7 Pa s the timescale for a 1 °C temperature difference is less than 40 s (with a lengthscale around 7 mm) and so it is unlikely that instabilities due to the mechanisms described in this paper would result. The temperature difference would have to be of order 7 °C for the timescale to be as long as 50 days. The corresponding lengthscale is again about $2\frac{1}{2}$ m. For the most viscous magmas, with viscosity 10^{11} Pa s, the timescale is again reduced, implying that the magma is more likely to remain stable. Even so, for larger, but still plausible, temperature differences such as 50 °C the critical timescale is nearly 2 years. In this case the lengthscale is just under 10 m. Provided that the timescale for the cooling of the sidewall of a magma chamber is less than 2 years and a temperature difference of at least 50 °C is involved then double-diffusive convection at the boundaries would always be expected. From this

we can see that double-diffusive convection from a sidewall could play a role in the dynamics of a broad range of magma chambers.

The instabilities described in this paper could also be important in many other situations that have not been discussed, such as icebergs melting into seas with both salinity and temperature gradients or solidifying alloys. This analysis only predicts the onset of instability and not necessarily the form the instabilities take or how they behave. If, for example, the fluid has a destabilizing temperature gradient then the bulk of the fluid could be unstable to nonlinear subcritical instabilities (Proctor 1981). The instabilities initiated at a boundary could in such circumstances trigger nonlinear instabilities in the bulk of the fluid, and the convection cells at the walls could then penetrate deep into the bulk of the fluid. However, for the case when both temperature and salinity gradients are stabilizing this would not be the case.

I would like to thank Professor R. S. J. Sparks for providing me with the data for magma contained in magma chambers.

REFERENCES

CHEN, C. F., BRIGGS, D. G. & WIRTZ, R. A. 1971 Stability of thermal convection in a salinity gradient due to lateral heating. *Intl J. Heat Mass Transfer* **14**, 57–65.

CHEN, C. F. & SKOK, M. W. 1974 Cellular convection in a salinity gradient along a heated inclined wall. *Intl J. Heat Mass Transfer* **17**, 51–60.

HART, J. E. 1971 On sideways diffusive instability. *J. Fluid Mech.* **49**, 279–288.

HART, J. E. 1973 Finite amplitude sideways diffusive convection. *J. Fluid Mech.* **59**, 47–64.

HOLYER, J. Y. 1983 Double-diffusive interleaving due to horizontal gradients. *J. Fluid Mech.* **137**, 347–362.

KERR, O. S. 1989 Heating a salinity gradient from a vertical sidewall: linear theory. *J. Fluid Mech.* **207**, 323–352 (referred to herein as I).

KERR, O. S. 1990 Heating a salinity gradient from a vertical sidewall: nonlinear theory. *J. Fluid Mech.* **217**, 529–546.

LINDEN, P. F. & WEBER, J. E. 1977 The formation of layers in a double-diffusive system with a sloping boundary. *J. Fluid Mech.* **81**, 757–773.

MCDOUGALL, T. J. 1985 Double-diffusive interleaving I. *J. Phys. Oceanogr.* **15**, 1532–1541.

NIINO, H. 1986 A linear theory of double-diffusive horizontal intrusions in a temperature-salinity front. *J. Fluid Mech.* **171**, 71–100.

PALIWAL, R. C. & CHEN, C. F. 1980 Double-diffusive instability in an inclined fluid layer. Part 2. Stability analysis. *J. Fluid Mech.* **98**, 769–785.

PHILLIPS, O. M. 1970 On flows induced by diffusion in a stably stratified fluid. *Deep-Sea Res.* **17**, 435–443.

PROCTOR, M. R. E. 1981 Steady subcritical thermohaline convection. *J. Fluid Mech.* **105**, 507–521.

SCHLADOW, S. G. & IMBERGER, J. 1987 Sidewall effects in a double diffusive system. *J. Geophys. Res.* **19**, 6501–6514.

STERN, M. E. 1967 Lateral mixing of water masses. *Deep-Sea Res.* **14**, 747–753.

THANGAM, S., ZEBIB, A. & CHEN, C. F. 1982 Double-diffusive convection in an inclined fluid layer. *J. Fluid Mech.* **116**, 363–378.

THORPE, S. A., HUTT, P. K. & SOULSBY, R. 1969 The effects of horizontal gradients on thermohaline convection. *J. Fluid Mech.* **38**, 375–400.

TSINOBER, A. & TANNY, J. 1986 Visualization of double-diffusive layers. In *Flow Visualization IV* (ed. Claude Venet), pp. 345–351. Hemisphere.

WUNSCH, C. 1970 On oceanic boundary mixing. *Deep-Sea Res.* **17**, 293–301.